Dissipation of Quasiclassical Turbulence in Superfluid ^{4}He

D. E. Zmeev,[1,2] P. M. Walmsley,[1] A. I. Golov,[1] P. V. E. McClintock,[2] S. N. Fisher,[2,*] and W. F. Vinen[3]

[1] *School of Physics and Astronomy, The University of Manchester, Manchester M13 9PL, UK*
[2] *Department of Physics, Lancaster University, Lancaster LA1 4YB, UK*
[3] *School of Physics and Astronomy, University of Birmingham, Birmingham B15 2TT, UK*

(Dated: March 6, 2015)

We compare the decay of turbulence in superfluid ^{4}He produced by a moving grid to the decay of turbulence created by either an impulsive spin-down to rest or by an intense ion injection. In all cases the vortex line density L decays at late time t as $L \propto t^{-3/2}$. At temperatures above 0.8 K, all methods result in the same rate of decay. Below 0.8 K, the spin-down turbulence maintains initial rotation and decays slower than grid turbulence and ion-jet turbulence. This may be due to a decoupling of the large-scale superfluid flow from the normal component at low temperatures, which changes its effective boundary condition from no-slip to slip.

PACS numbers: 47.80.Jk, 67.25.dk, 47.27.-i

Turbulence is a common state of flow in classical fluids, with great importance from atmospheric systems to aircraft design. So far, satisfactory understanding is only achieved for homogeneous and isotropic turbulence (HIT) [1]. HIT can be approximately obtained in the wake of a flow past a grid [2], although it might still be strongly modified by the container geometry [3, 4]. Grid turbulence in superfluid ^{4}He was obtained [5, 6], but not at temperatures below 1 K due to technical difficulties. Yet, the low-temperature regime enjoys a special interest, as the thermal excitations (the normal component) are essentially absent. Turbulence of the superfluid is made of a chaotic motion of tangled topological defects of the superfluid order parameter field – quantized vortices – each carrying the same circulation equal to the ratio of the Planck's constant to the mass of a ^{4}He atom: $\kappa = h\,m^{-1}$. It is called Quantum Turbulence (QT), as it is essentially a macroscopic quantum phenomenon. QT decays even at the lowest temperatures, but the mechanisms of dissipation in superfluid ^{4}He – thought to be the radiation of phonons by Kelvin waves (perturbations of vortex lines) with wavelength $\sim 10^{-7}$ cm [7] and also of small ballistic vortex loops that can carry energy away [8–11] – only operate at very small length scales. Existing theories [15–19] of QT decay are applicable to homogeneous isotropic QT (HIQT), for which only sparse experimental data are available in the interesting ultra-low temperature limit.

In this Letter we report the best-yet realisation of HIQT in the $T \to 0$ limit. We measure the free decay of grid turbulence and compare the results with both theory and experiments using other methods, thereby gaining valuable insights into the underlying processes.

When QT is generated by large-scale flow, on length scales much greater than the mean intervortex distance $\ell = L^{-1/2}$, where L is the length of vortex lines per unit volume, then the energy is predominantly contained in flow at the largest length scales $\gg \ell$. In this case QT is called *quasiclassical* [12], as quantization of vorticity becomes unimportant, and the coarse-grained velocity field is expected to obey the Euler equation. It is believed that this energy cascades towards the smaller length scales via a classical hydrodynamic cascade, followed, at length scales $\leq \ell$, by a 'quantum cascade' that involves reconnections and Kelvin waves on discrete vortex lines. Existing theories [15–19] of these processes in HIQT all assume that the dominant contribution to L is at quantum mesoscales $\sim \ell$, but they differ in detail. For self-similar flows, assuming that the rate of dissipation of flow energy per unit mass, $\mathcal{E}$, only depends on L and κ, dimensional considerations demand

$$\dot{\mathcal{E}} = -\zeta \kappa^3 L^2. \tag{1}$$

Here, the 'non-dimensional effective kinematic viscosity' $\zeta \sim 1$ (the more conventional 'effective kinematic viscosity' is $\nu' \equiv \zeta\kappa$). At medium temperatures $1.0 \lesssim T \lesssim 1.6$ K, it reflects the dissipation through the interaction of vortices with thermal excitations (expressed through the 'mutual friction parameter' $\alpha(T)$), while in the limit $T \to 0$ ($T \lesssim 0.5$ K) it characterizes the efficiency of the tangle of vortex lines in maintaining the energy cascade down to the dissipative length scale. As there is no microscopic derivation of (1), it remains unclear whether the value of ζ is the same for HIQT of any spectrum, or depends on the type of flow. For instance, $\zeta = 0.08$ was measured [20] for Vinen ('ultraquantum', i. e. without flow at classical length scales $> \ell$) QT at $T \to 0$, while the analysis of the decay of QT generated by spin-down at $T \to 0$ apparently revealed $\zeta \approx 0.003$ [21]. The latter was heralded as evidence for the poor efficiency of the energy cascade in quasiclassical QT due to the 'bottleneck' between the classical and quantum length-scales [16]. However, recent experiments in a rotating container revealed vanishing traction by the container walls on turbulent superfluid ^{3}He at low temperatures when $\alpha < 10^{-3}$, resulting in a long-lived rotating state [22]. This cast doubts on the interpretation of ^{4}He spin-down turbulence as being HIQT [21] and pushed for new experiments with truly HIQT.

Thus, the goal of this work was to measure and compare the decay rates of different types of turbulent flow, including those generated by a towed grid and impulsive spin-down, in a broad range of temperatures. To determine the value of ζ, one has to know both L and $\dot{\mathcal{E}}$ in (1). With our technique of free decay, the injected energy flux, $-\dot{\mathcal{E}}$, is controlled by the size of the largest energy-containing eddy and its lifetime. In fact, (1) with a meaningful ζ can only be applied for homogeneous turbulence while, for bound inhomogeneous flows, only an integral rate of energy dissipation can be measured together with some averaged value of vortex line density. We will hence assume that (1) relates average $\dot{\mathcal{E}}$ and L through some integral ζ.

The energy per unit mass of helium in the energy-containing eddies with velocity amplitude u is $\mathcal{E} = \xi u^2$, where $\xi \lesssim 1/2$. Their length scale λ is saturated by the container size d, $\lambda = \beta d$, where $\beta \sim 1$. We assume that, as in classical turbulence, the energy is released within the life time τ of order the turn-over time $\sim \lambda u^{-1}$, i. e. $\tau = \theta \lambda u^{-1}$, where $\theta \sim 1$. In the quasi-steady regime, the energy flux fed into the cascade is hence $-\dot{\mathcal{E}} = \mathcal{E}\tau^{-1}$ or

$$-2\xi u\dot{u} = \xi u^3 \theta^{-1}\beta^{-1}d^{-1}. \tag{2}$$

Its solution at late time t is

$$\mathcal{E}(t) = 4\xi\theta^2\beta^2 d^2 t^{-2}, \tag{3}$$

$$\tau(t) = t/2. \tag{4}$$

After plugging (3) into (1), we arrive at

$$L(t) \sim Ad(\kappa t)^{-3/2}, \tag{5}$$

where $A \equiv (8\xi)^{1/2}\theta\beta\zeta^{-1/2} \sim 1$. This is the $L \propto t^{-3/2}$ free decay that was observed in many experiments [6, 13, 14, 20, 21, 23] and numerical simulations [24].

Our experiments were conducted in ultra-pure [25, 26] ^{4}He at pressure 0.1 bar filling the volume shown in Fig. 1: a 90 ° section of an earthed annular channel with an inner wall radius of curvature equal to 2.75 cm and of rectangular cross-section 1.8 cm (horizontal)×1.7 cm (vertical). A brass grid (1.5 cm×1.5 cm) could be electromagnetically driven at a constant velocity from one end of the channel to the other. The operating principle of the device and its performance characteristics are described elsewhere [27]. The vortex line detector had two parts, which were fitted into the identical openings in the opposite vertical walls of the channel: the injector and collector assemblies. The injector consisted of a sharp tungsten tip [28] with a 92 % open tungsten grid in front of it. The collector was a brass disk with the same type of grid in front of it. By applying pulses of high voltage (400-600 V, 0.1 s long) to the injector tip, we produced current pulses (typically, 0.1 s long and of $I \lesssim 300$ pA in magnitude). In liquid helium, excess electrons form microscopic bubbles. At

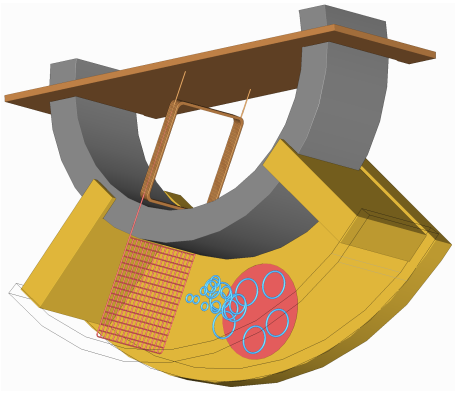

FIG. 1. Experimental setup [27]. The grid could be moved from one end of the channel to the other. Vortices in the channel were detected using either CVRs (drawn not to scale) at $T \leq 0.7$ K or bare negative ions at $T \geq 0.7$ K, which propagated across the channel from the injector on the left to the collector on the right (the injector and collector, as well as the front and bottom walls of the channel, are not shown). The assembly was housed inside a sealed volume, thermally anchored to the mixing chamber of a rotating dilution refrigerator that could be rotated about the vertical axis.

temperatures below 0.7 K they are attached to quantized vortex rings, thus forming charged vortex rings (CVRs). Both CVRs and bare electron bubbles, while moving in the vicinity of a vortex line, either change their trajectory or become trapped on the vortex lines. Hence, by measuring the attenuation of the electric current arriving at the collector, $\gamma(L) = \ln[I(0)/I(L)]$, we could characterize the vortex tangle in the experimental volume.

The presence of rotation of the vortex tangle causes a sideway deflection of the beam of CVRs via the Coriolis effect. In the vortex detector, the guiding electric field could be made either converging (by grounding the injector grid while applying positive potential to the collector grid, typically +30 V) or diverging (by grounding the collector grid while applying negative potential to the injector grid, typically −60 V). The former assures that all injected CVRs end up within the collector disk; a small deflection of the beam off axis causing no change in the collector current. The latter, on the other hand, widens the beam of the CVRs beyond the diameter of the collector. By positioning the injector slightly off the vertical symmetry plane, we hence had a different response of the total collector current to small sideways deflections of the ions. We thus could use the detector in two regimes: (i) vortex line density meter (L-meter) with converging field; (ii) detector of the vertical polarization of vorticity (P-detector) with diverging field. In both regimes, the detector was calibrated in steady rotation at fixed values of the angular velocity Ω, when the experimetal volume is filled with an array of rectilinear vortices of the equilibrium density $L = 2\Omega/\kappa$.

In the P-detector regime, the current attenuation,

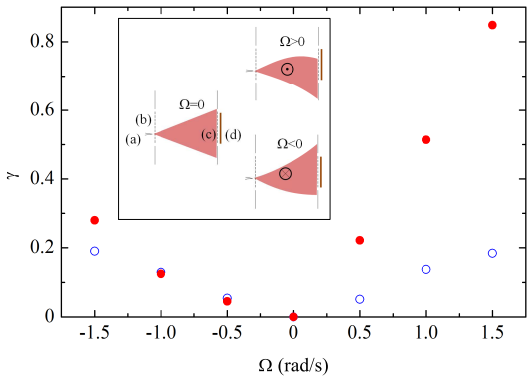

FIG. 2. Calibration of the vortex detector in the L-meter regime (open circles) and P-detector regime (filled circles) in steady rotation. Inset shows a sketch (view from above) of the P-detector: the beam of CVRs is deflected either towards or away from the collector depending on the sense of rotation. Parts of the vortex detector: (a) tungsten tip, (b) injector grid, (c) collector grid, (d) collector.

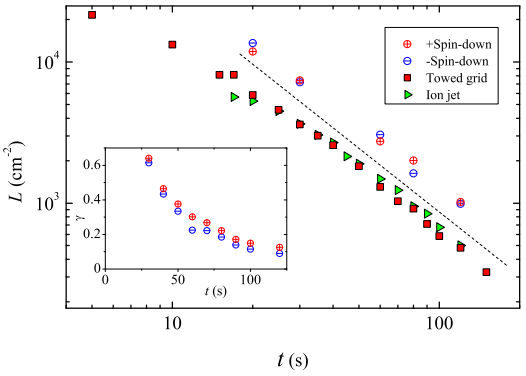

FIG. 3. Decay of turbulence generated by various means as measured by the L-meter: '+Spin-down' – spin-down from $\Omega = +1.5$ rad/s, '-Spin-down' – spin-down from $\Omega = -1.5$ rad/s, 'Towed grid' – grid moving at 15 cm/s, 'Ion jet' – negative ion injection at a current of 700 pA lasting for 100 s. Dashed line shows the $t^{-3/2}$ dependence. Inset: decay of turbulence generated by spin-down from $\Omega = \pm 1.5$ rad/s as measured by the P-detector. $T = 80$ mK.

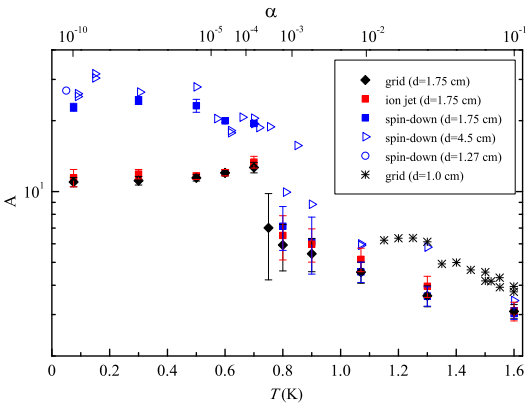

FIG. 4. The values of the fitting parameter $A = L(t)d^{-1}(\kappa t)^{3/2}$ vs. temperature (values of the mutual friction parameter $\alpha(T)$ are shown at the top). Measurements by Stalp *et al.* [13] are shown by asterisks for comparison.

γ, responded differently to opposite senses of rotation: $\gamma(\Omega) \neq \gamma(-\Omega)$, because the centre of the wide beam of CVRs was deflected either towards or away from the collector, as the cartoon inset of Fig. 2 shows. More precisely, $\gamma(\Omega) > \gamma(-\Omega)$ for $\Omega > 0$, as filled circles in Fig. 2 show. The P-detector, therefore, could be used to detect the sign of the vertical polarization of the vortex tangle. Our experiments at $T < 0.5$ K show that the P-detector can distinguish between spin-down turbulence produced from the initial states with $\Omega = +1.5$ rad/s and $\Omega = -1.5$ rad/s (inset in Fig. 3). Moreover, turbulence generated from the state with a positive Ω is characterized by a greater value of γ compared to the state produced from $\Omega < 0$, as is the case in steady rotation (Fig. 2), when vertical polarization is the highest. Thus memory about the initial state in spin-down turbulence is retained down to late times of turbulence decay – presumably in the form of a slowly-rotating central core, weakly interacting with the turbulence near the walls.

In the L-meter regime, the electric current attenuation did not depend on the sense of rotation, $\gamma(\Omega) = \gamma(-\Omega)$ (open circles in Fig. 2), and the vortex line density is given by [29]

$$L = \gamma \sigma^{-1} d^{-1}, \tag{6}$$

where σ is the mean scattering diameter for the given guiding field.

We investigated the decay of turbulence generated by three different methods: towing the grid through the channel [30], impulsive spin-down from uniform rotation to rest, and injection of relatively high electric currents for long periods of time (~ 1 nA for 100 s; this produces a jet, propagating into the experimental volume [20]). After generation, $L(t)$ was probed at a delay t. Each realisation was probed only once to avoid distortion of the turbulent flow by the probing pulses. For each method, we forced QT sufficiently hard, so that the late-time decay was the same, independent of the intensity of forcing (e. g. if the grid moved faster than ≈ 5 cm/s). In the experiments with grid turbulence the values $L(t)$ at late times did not depend on how many times in succession (1, 2, 3 or 10) the grid was towed through the channel, nor did it depend on the grid mesh sizes used (0.75 mm and 3 mm). In the experiments with rotation the grid was parked at one end of the channel.

For all temperatures and all methods of turbulence generation, the decay of vortex line density followed $L \propto t^{-3/2}$ at late times, as shown in Fig. 3. We fitted them to (5), and the resulting values of $A(T)$ are plotted in Fig. 4. We also compare these with the experimental values of $A(T)$ for grid turbulence (square channel,

$d = 1.27\,\mathrm{cm}$) [6, 13] and spin-down turbulence (cubic cell, $d = 4.5\,\mathrm{cm}$ [21] and rectangular cell, $d = 1.27\,\mathrm{cm}$ [12]). One can see that at temperatures above 0.8 K, corresponding to $\alpha > 10^{-3}$, the values of $A(T)$ for all methods of turbulence generation in our container agree with each other and also, within their scatter, with previous experiments. However, at $T < 0.8\,\mathrm{K}$ $A(T)$ jumps towards either of two zero-temperature limits: $A(0) \approx 11$ for both the ion-jet and grid-generated turbulence, while $A(0) \approx 23$ for the spin-down turbulence. We would thus conclude that at $T > 0.8\,\mathrm{K}$ the late-time turbulence is the same whatever the initial flow, i. e. approximatelly isotropic and homogeneous. This implies that the leftovers of the initial flow pattern (say, rotation following spin-down) disappear within the transient time of order 20 s. But at lower temperatures, the spin-down turbulence is different from that for other methods at all times; this seems to be correlated with our observation that the memory of initial rotation is retained during the late-time decay [36].

The reason for retaining rotation might be a switch to effectively 'slip' boundary condition (BC) at $T < 0.8\,\mathrm{K}$, caused by the decoupling of the superfluid component from the normal component at large length scales and time scales of order the decay time. During the transient following the spin-down of a rectangular cell, much of the fluid's initial angular momentum is transfered to the walls through pressure fluctuations, eventually creating turbulence with a broad distribution of length scales. At late times, when, as we suppose, the remains of that angular momentum survive only in the core near the axis, the pressure fluctuations at walls become inefficient, and only the traction at the walls exerts torque. With slip BC this torque vanishes (if one neglects the surface friction due to the interaction of vortex lines with wall roughness [31, 32] and gridded orifices). For laminar flow, the relaxation time for coupling between the superfluid and a stationary normal component is $\sim [\alpha(T)\kappa L]^{-1}$. With decreasing temperature, it rapidly increases and should be compared to the lifetime of energy-containing eddies (4): the cross-over from the limit of coupled to uncoupled components would thus be expected at $\alpha \sim 2[\kappa t L(t)]^{-1}$. For typical $L(t) \sim 10^4\,\mathrm{cm}^{-2}$ at $t \sim 20\,\mathrm{s}$, this corresponds to $\alpha(T) \sim 10^{-2}$, i. e. to $T \sim 1.1\,\mathrm{K}$. However, in a turbulent state, the locally-enhanced density of vortex lines near walls might enhance the mutual friction force, hence allowing the cross-over to occur at smaller values of $\alpha(T)$. Furthermore, as the mechanical forcing is expected to affect the large-scale superfluid and normal flow in a similar manner, these flows might be generated nearly fully-coupled from the outset; this might further ease the condition for coupling and allow the cross-over to 'slip' BC to occur at a lower temperature. Note that rotation of superfluid ^{3}He was also found to decouple from container walls when $\alpha \lesssim 10^{-3}$ [22, 34, 35].

As in the classical case [33], the residual rotation should slow down the cascade of energy to smaller eddies and thus increase the value of θ. Hence, according to (5), this can explain the fact that, at the same decay time t, the vortex line density $L(t)$ is higher for spin-down turbulence than for grid turbulence. It is also comforting to see that spin-down turbulences in containers with three different d all returned similar zero-temperature $A \equiv L(\kappa t)^{3/2} d^{-1}$ in Fig. 4 (different blue symbols), as predicted by (5).

Let us now discuss the possible effect of BC on the decay rate of grid turbulence. Far from walls, the dynamics of the superfluid eddies (whether coupled to the low-viscosity normal component at $T \gtrsim 1\,\mathrm{K}$ or decoupled from the vanishing normal component at $T \lesssim 1\,\mathrm{K}$) at classical length scales is expected to be identical [37]. However, this is not the case for the energy-containing eddies in a container, because they are affected by walls. No-slip BC would speed-up the breakdown of eddies through the diffusion of vorticity via eddy viscosity and thus decrease the parameter θ relative to its bulk value for eddies of the same size; while slip BC might actually increase the value of θ. The effective size of the largest eddies in a container might also be greater for slip BC, which will be reflected in a larger value of β. Either effect could thus explain an increase of the parameter $A \propto \beta\theta\zeta^{-1/2}$ if BC becomes of slip type below 0.8 K – even if the effective kinematic viscosity $\zeta(T)$ stayed the same.

As the values of the parameters ξ, β and θ for a container of particular shape and BC are unknown, it is impossible to determine the accurate value of ζ from A. Stalp *et al.* [6] introduced an approach, in which they assumed that the energy spectrum in the space of wavenumbers k is meaningful and equal to the Kolmogorov spectrum $E_k = C\epsilon^{2/5}k^{-5/3}$ (with $C \approx 1.5$) all the way down to the the cut-off wavenumber $k_1 \sim d^{-1}$. In Supplementary Notes [38] we show that these assumptions are unrealistic, and one hence cannot expect accurate values of ζ from this approach. Yet, we quote its result for $T = 0$: for slip BC (for which $k_1 = \pi/d$), the value $A(0) = 11$ for grid turbulence (Fig. 4) would correspond to $\zeta(0) \approx 0.08$. This basically coincides with values $\zeta(0) = 0.08$–0.09 measured experimentally [20, 39] and $\zeta(0) = 0.06$–0.10 calculated numerically [40, 41] for Vinen QT, in which classical degrees of freedom are not excited – thus suggesting that there is no bottleneck between the classical and quantum cascades. It seems the same bulk parameter $\zeta(T)$ characterizes the efficiency of quantum cascades in HIQT for different spectra.

To conclude, by towing a grid through superfluid helium in the zero-temperature limit, we have produced the best-yet realization of quasiclassical HIQT filling a container, and measured its decay rate. The low-temperature decay of HIQT follows the law $L \propto t^{-3/2}$, observed for all quasi-classical QT, but its decay is markedly faster than that of the turbulence generated

by an impulsive spin-down to rest. The latter may be due to the change of the effective BC from no-slip to slip because of the loss of traction at the container walls below 0.8 K. As a result, the spin-down flow maintains rotation, and is responsible for the slowing-down of the decay of turbulence.

This work was supported through the Materials World Network program by the Engineering and Physical Sciences Research Council (Grant No. EP/H04762X/1). P. M. W. is indebted to EPSRC for the Career Acceleration Fellowship (Grant No. EP/I003738/1). We thank V. B. Eltsov and V. S. L'vov for fruitful discussions.

* Deceased 4 January 2015.

[1] U. Frisch. Turbulence: The Legacy of A. N. Kolmogorov. Cambridge University Press, 1995.

[2] G. K. Batchelor, The Theory of Homogeneous Turbulence (Cambridge University Press, Cambridge, 1953).

[3] In a container with classical fluid, different protocols of initiating turbulence can result in different large-scale flows (see [4] and references therein).

[4] S. G. Huisman, R. C. A. van der Veen, C. Sun and D. Lohse, Nature Comm. **5**, 3820 (2014).

[5] M. R. Smith, R. J. Donnelly, N. Goldenfeld, and W. F. Vinen, Phys. Rev. Lett. **71**, 2583 (1993).

[6] S. R. Stalp, L. Skrbek, and R. J. Donnelly, Phys. Rev. Lett. **82**, 4831 (1999).

[7] W. F. Vinen, Phys. Rev. B **64**, 134520 (2001).

[8] B. V. Svistunov, Phys. Rev. B **52**, 3647 (1995).

[9] S. K. Nemirovskii Phys. Rev. B **81**, 064512 (2010).

[10] C. F. Barenghi and D. C. Samuels, Phys. Rev. Lett. 89, 155302 (2002).

[11] M. Kursa, K. Bajer, and T. Lipniacki, Phys. Rev. B **83**, 014515 (2011).

[12] P. M. Walmsley, D. E. Zmeev, F. Pakpour, and A. I. Golov, Proc. Natl. Acad. Sci. USA **111**, 4691 (2014).

[13] S. R. Stalp *et al.*, Phys. Fluids **14**, 1377 (2002).

[14] J. J. Niemela, K. R. Sreenivasan, and R. J. Donnelly, JLTP **138**, 537 (2005).

[15] C. F. Barenghi, V. S. L'vov, and P.-E. Roche, Proc. Natl. Acad. Sci. USA **111**, 4683 (2014).

[16] V. S. Lvov, S. V. Nazarenko, O. Rudenko, Phys. Rev. B **76**, 024520 (2007).

[17] E. V. Kozik and B. V. Svistunov , Phys. Rev. Lett. **100**, 195302 (2008).

[18] E. V. Kozik and B. V. Svistunov, J. Low Temp. Phys. **156**, 215 (2010).

[19] E. B. Sonin, Phys. Rev. B **85**, 104516 (2012).

[20] P. M. Walmsley and A. I. Golov, Phys. Rev. Lett. **100**, 245301 (2008).

[21] P. M. Walmsley, A. I. Golov, H. E. Hall, A. A. Levchenko, and W. F. Vinen, Phys. Rev. Lett. **99**, 265302 (2007).

[22] J. J. Hosio *et al.*, Nature Comm. **4**, 1614 (2013).

[23] D. I. Bradley *et al.*, Phys. Rev. Lett. **96**, 035301 (2006).

[24] V. B. Eltsov *et al.*, J. Low Temp. Phys. **161**, 474 (2010).

[25] ^{4}He gas with ^{3}He concentration 2×10^{-11} was obtained using the heat-flush technique [26].

[26] P. C. Hendry and P. V. E. McClintock, Cryogenics **27**, 131 (1987).

[27] D. E. Zmeev, J. Low Temp. Phys. **175**, 480 (2014).

[28] A. Golov and H. Ishimoto, J. Low Temp. Phys. **113**, 957 (1998).

[29] K. W. Schwarz and R. J. Donnelly, Phys. Rev. Lett. **17**, 1088 (1966).

[30] We have also investigated turbulence generated by the same grid oscillating with amplitude ~ 0.6 mm and frequency ~ 15 Hz, 2 cm away from the detector for typically 100 s. $L(t)$ was measured after the oscillations were stopped. Although turbulence produced in this way is initially highly inhomogeneous (with L decreasing with distance from the grid), at $t > 100$ s $L(t)$ showed the same late-time decay as after a towed grid (Fig. 3).

[31] P. W. Adams, M. Cieplak and W. I. Glaberson, Phys. Rev. **32**, 171 (1985).

[32] R. J. Zieve, C. M. Frei, D. L. Wolfson, Phys. Rev. B **86**, 174504 (2012).

[33] C. Lamriben, P.-P. Cortet, F. Moisy, and L. R. M. Maas, Phys. Fluids **23**, 015102 (2011).

[34] V. Eltsov, R. Hanninen and M. Krusius, PNAS **111**, 4711 (2014).

[35] J. J. Hosio *et al.*, Phys. Rev. Lett. **107**, 135302 (2011).

[36] The difference between $\gamma(t)$ after spin-down from +1.5 rad/s and -1.5 rad/s (from inset in Fig. 3) is roughly constant, $\gamma_+ - \gamma_- = 0.40 \pm 0.15$, for $30\,\mathrm{s} \le t \le 120\,\mathrm{s}$. Using the experimental $\gamma(\Omega)$ from Fig. 2 and assuming that the contributions to $\gamma \ll 1$ from the scatttering of CVRs off vortex lines and from the deflection of the beam of CVRs by the Coriolis force are additive, we estimate the residual angular velocity of the rotating central core at late time $30\,\mathrm{s} \le t \le 120\,\mathrm{s}$ as $\Omega_0 \sim 0.08$ rad/s. The contribution from the polarised component of this rotating vortex tangle, $2\Omega_0/\kappa \sim 1.6 \times 10^2\,\mathrm{cm}^{-2}$ is negligible compared to the total $L(t) \ge 10^3\,\mathrm{cm}^{-2}$ at all times t studied.

[37] W. F. Vinen, Phys. Rev. B **61**, 1410 (2000).

[38] Supplementary Notes to this Letter.

[39] We have also generated Vinen turbulence in this cell, using the method of tangling a small packet of charged vortex rings as in [20] and observed the decay $L = 1.6 \times 10^4\,\mathrm{s\,cm^{-2}}t^{-1}$, which is close to $L = 1.3 \times 10^4\,\mathrm{s\,cm^{-2}}t^{-1}$ observed in a cubic cell of 4.5 cm side [20]. The independence of the container size for this type of turbulence is indeed expected from theory: $L \approx 1.2\kappa^{-1}\zeta^{-1}t^{-1}$ [20].

[40] M. Tsubota, T. Araki, and S. K. Nemirovskii, Phys. Rev. B **62**, 11751 (2000).

[41] L. Kondaurova, V. Lvov, A. Pomyalov, and I. Procaccia, Phys. Rev. B **90**, 094501 (2014).